



# *Cistanche tubulosa* Phenylethanoid Glycosides Induce Apoptosis of Hepatocellular Carcinoma Cells by Mitochondria-Dependent and MAPK Pathways and Enhance Antitumor Effect through Combination with Cisplatin

Integrative Cancer Therapies  
Volume 20: 1–19  
© The Author(s) 2021  
Article reuse guidelines:  
sagepub.com/journals-permissions  
DOI: 10.1177/15347354211013085  
journals.sagepub.com/home/ict  


Pengfei Yuan, BSc<sup>1</sup>, Changshuang Fu, MSc<sup>1</sup>, Yi Yang, PhD<sup>1</sup>, Aipire Adila, PhD<sup>1</sup>, Fangfang Zhou, MSc<sup>1</sup>, Xianxian Wei, MSc<sup>1</sup>, Weilan Wang, PhD<sup>1</sup>, Jie Lv, PhD<sup>1</sup>, Yijie Li, PhD<sup>1</sup>, Lijie Xia, PhD<sup>1</sup> , and Jinyao Li, PhD<sup>1</sup>

## Abstract

*Cistanche tubulosa* is a type of Chinese herbal medicine and exerts various biological functions. Previous studies have been demonstrated that *Cistanche tubulosa* phenylethanoid glycosides (CTPG) exhibit antitumor effects on a variety of tumor cells. However, the antitumor effects of CTPG on HepG2 and BEL-7404 hepatocellular carcinoma (HCC) cells are still elusive. Our study showed that CTPG significantly inhibited the growth of HepG2 and BEL-7404 cells through the induction of cell cycle arrest and apoptosis, which was associated with the activation of MAPK pathways characterized by the up-regulated phosphorylation of p38, JNK, and ERK1/2 and mitochondria-dependent pathway characterized by the reduction of mitochondrial membrane potential. The release of cytochrome c and the cleavage of caspase-3, -7, -9, and PARP were subsequently increased by CTPG treatment. Moreover, CTPG significantly suppressed the migration of HepG2 through reducing the levels of matrix metalloproteinase-2 and vascular endothelial growth factor. Interestingly, CTPG not only enhanced the proliferation of splenocytes but also reduced the apoptosis of splenocytes induced by cisplatin. In H22 tumor mouse model, CTPG combined with cisplatin further inhibited the growth of H22 cells and reduced the side effects of cisplatin. Taken together, CTPG inhibited the growth of HCC through direct antitumor effect and indirect immunoenhancement effect, and improved the antitumor efficacy of cisplatin.

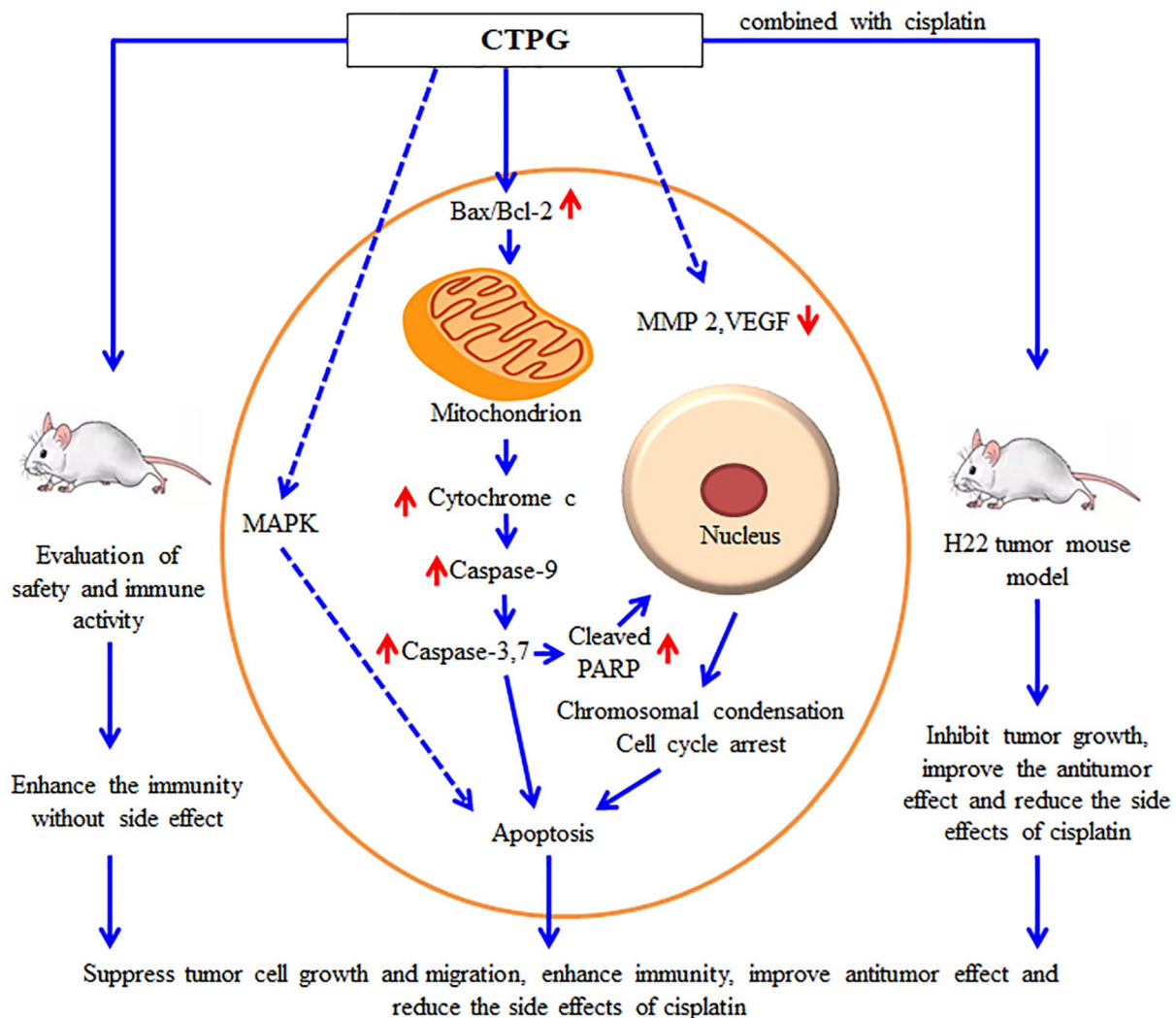
## Keywords

*Cistanche tubulosa* phenylethanoid glycosides, apoptosis, MAPK pathway, mitochondria-dependent pathway, cisplatin, immunoenhancement

Submitted December 30, 2020; revised April 7, 2021; accepted April 8, 2021



## Graphical Abstract



## Introduction

Liver cancer was predicted to be the sixth most commonly diagnosed cancer and the fourth leading cause of cancer death worldwide in 2018, with about 841 000 new cases and 782 000 deaths annually in South-Eastern Asia (Mongolia, Cambodia, and Vietnam).<sup>1</sup> In China, liver cancer was the third leading cause of cancer-related death in 2015.<sup>2</sup> More

than 90% of primary liver cancers are hepatocellular carcinoma (HCC) throughout the world. Currently, hepatectomy, liver transplantation, and percutaneous ablation are the main methods for the treatment of HCC. Unfortunately, these treatments are effective for 30% patients diagnosed with early liver cancer, while patients diagnosed as advanced liver cancer (accounting for 40%) have to rely on palliative

<sup>1</sup>Xinjiang University, Urumqi, Xinjiang, China

## Corresponding Authors:

Jinyao Li, Xinjiang Key Laboratory of Biological Resources and Genetic Engineering, College of Life Science and Technology, Xinjiang University, Urumqi 830046, China.

Email: ljyxju@xju.edu.cn

Lijie Xia, Xinjiang Key Laboratory of Biological Resources and Genetic Engineering, College of Life Science and Technology, Xinjiang University, Urumqi 830046, China.

Email: xialijie1219@163.com

treatment to extend their survival time.<sup>3,4</sup> Sorafenib in combination with hepatic arterial chemoembolism is an important and common palliative therapy for most patients with advanced HCC in the Asia-Pacific region.<sup>5</sup> Sorafenib, approved by FDA in 2006 for the treatment of advanced liver cancer, is a multiple kinase inhibitor that inhibits tumor cell proliferation and vascular production and promotes tumor cell apoptosis. Sorafenib significantly extends the patient's survival time by 3 to 5 months but has serious side effects and is closely related to the occurrence of drug resistance.<sup>6</sup> Therefore, it is urgent to develop new drugs or strategies for HCC.

Traditional Chinese medicine (TCM) alone or in combination with other strategies has been used to treat HCC and has shown clinical benefits including extended survival time, improved life quality, reduced adverse reactions, and so on.<sup>7,8</sup> *Cistanche* is a TCM containing phenylethanoid glycosides (PhGs), iridoids, lignin, and polysaccharides which has various biological functions, such as anti-oxidation, anti-inflammation, anti-aging, memory enhancement, and immune enhancement functions.<sup>9</sup> PhGs have been considered as the major active components of *Cistanche*, and have multiple functions including anti-oxidation, anti-inflammation, anti-apoptosis, hepatoprotection, and neuroprotection.<sup>10-12</sup> Our group had reported that *Cistanche tubulosa* phenylethanoid glycosides (CTPG) could inhibit the growth of melanoma B16-F10 cells, esophageal carcinoma Eca-109 cells, and HCC H22 cells through extrinsic or intrinsic signaling pathways in vitro or in vivo; in addition, CTPG had an immunostimulatory effect.<sup>13-15</sup>

In this study, we investigated the antitumor effect and mechanism of CTPG on HepG2 and BEL-7404 cells in vitro, analyzed the immunomodulatory function of CTPG in vitro and in vivo, and further evaluated the therapeutic effect of CTPG combined with the chemotherapy drug cisplatin on HCC H22 tumor mice in vivo. We found that CTPG could inhibit the growth of HepG2 and BEL-7404 cells through mitochondria-dependent apoptosis and the MAPK signaling pathway. CTPG significantly inhibited the migration of HepG2 cells by reducing the levels of matrix metalloproteinase-2 (MMP-2) and vascular endothelial growth factor (VEGF). In addition, CTPG promoted the proliferation and activation of immune cells, and enhanced the immunity of mice. Importantly, CTPG combined with cisplatin can further inhibit the growth of H22 cells in vivo and reduced the side effects of cisplatin.

## Materials and Methods

### Animals

About 6 to 8 week old male BALB/c, Kunming mice, and female C57BL/6 mice were purchased from the Animal Laboratory Center, Xinjiang Medical University (Urumqi, Xinjiang, China) and housed in an animal facility of

Xinjiang University with the room temperature (RT) of  $25 \pm 3^\circ\text{C}$ , and a 12/12 hours light-dark period.

### Cell Lines and Cell Culture

The murine H22 cells were purchased from Procell Life Science & Technology Co., Ltd. (Wuhan, Hubei, China) and human HCC HepG2 and BEL-7404 cells were obtained from the Xinjiang Key Laboratory of Biological Resources and Genetic Engineering, Xinjiang University (Urumqi, Xinjiang, China) and cultured in RPMI 1640 medium (Gibco, USA) or Dulbecco's modified Eagle's medium (DMEM) (Gibco) containing 10% heat-inactivated fetal bovine serum (MRC, China), 1% L-glutamine (100 mM), 100 U/mL penicillin, and 100  $\mu\text{g}/\text{mL}$  streptomycin at  $37^\circ\text{C}$  in a humidified atmosphere of 5%  $\text{CO}_2$ .

### High Performance Liquid Chromatography (HPLC)

The major compounds of CTPG (Upbio Tech Co., Ltd., Shanghai, China) were qualified and quantified by HPLC as previously reported.<sup>13</sup> A ZORBAX SB-C18 Column ( $250 \times 4.6 \text{ mm}$ ;  $5 \mu\text{m}$ ) was used and the mobile phase consisted of 0.2% formic acid solution and methanol with a gradient from 23% to 31%. A total of 10  $\mu\text{L}$  sample was injected and detected at 330 nm. The echinacoside and acteoside standards (Yuanye, Shanghai, China) were used to analyze the components of CTPG.

### Analysis of Cell Viability

The antitumor effects of CTPG on HepG2 and BEL-7404 cells were assessed using MTT (3-(4, 5-dimethyl-2-thiazolyl)-2, 5-diphenyl-2-H-tetrazolium bromide). HepG2 and BEL-7404 cells were plated into 96-well plates ( $5 \times 10^4$  cells/well) and treated with 0, 200, 400, and 600  $\mu\text{g}/\text{mL}$  CTPG for 24 and 48 hours, respectively, after 24 hours of incubation at  $37^\circ\text{C}$ . About 35  $\mu\text{g}/\text{mL}$  cisplatin (Yuanye) was used as positive control. Then 100  $\mu\text{L}$  MTT (0.5 mg/mL, diluted by medium without FBS medium) was added to each well and cultured for 3 hours at  $37^\circ\text{C}$  and 5%  $\text{CO}_2$ . After incubation, the plates were centrifuged at 1200 rpm for 7 minutes, the medium was removed and 200  $\mu\text{g}/\text{mL}$  DMSO was added to each well to dissolve the formed formazan crystals. The OD490 values were measured by a 96-well microplate reader (Bio-Rad Laboratories, CA, USA). To evaluate the effects of CTPG on splenocytes, the cells were isolated from C57BL/6 mice and plated into 96-well plates at a density of  $1 \times 10^5$  cells/well. Splenocytes were treated with 0, 200, 400, and 600  $\mu\text{g}/\text{mL}$  for 24, 48, and 72 hours, respectively. The cell viability was calculated as the followed formula: Cell viability (%) =  $(\text{OD}_{\text{treated}} / \text{OD}_{\text{untreated}}) \times 100\%$ .

### Detection of Ki-67

Detection of Ki-67 was done according to our previous study.<sup>16</sup> In brief, BEL-7404 cells were treated with different concentrations (0, 200, 400, and 600  $\mu\text{g}/\text{mL}$ ) of CTPG or cisplatin (35  $\mu\text{g}/\text{mL}$ ). After 24 hours, cells were harvested and washed with PBS, then fixed and permeabilized with Foxp3 Staining Buffer Set (eBioscience, USA) according to the manufacturer's instructions. Intracellular staining was performed using FITC conjugated *Ki-67* antibody (BD Biosciences, San Jose, CA, USA) for 15 minutes at RT. The samples were analyzed by flow cytometry (BD FACSCalibur, CA, USA).

### Analysis of Cell Apoptosis and Cell Cycle

HepG2 and BEL-7404 cells were seeded at a density of  $2.5 \times 10^5$  cells/dish and incubated at 37°C overnight. Cells were trypsinized and harvested by centrifugation after treatment with various concentrations of CTPG or pretreated with caspase inhibitor (Z-VAD-FMK) or caspase-3 inhibitor (Ac-DEVD-CHO) (Beyotime, China) for 2 hours before CTPG treatment. After 24 hours, apoptosis was detected by flow cytometry. In brief, the collected cells were washed with cold PBS (Gibco) and resuspended in annexin-binding buffer with 2.5  $\mu\text{L}$  Annexin V-FITC and 5  $\mu\text{L}$  PI-PE Staining Solution (Solarbio, Beijing, China), and then cells were incubated at RT in the dark for 15 minutes. For analysis of the cell cycle distribution, cells were harvested after CTPG treatment and fixed in cold 70% ethanol at 4°C for 30 minutes. Cells were stained with PI (BD Biosciences) in the dark for 30 minutes. Samples were analyzed by flow cytometer (BD FACSCalibur). Expression levels of cell apoptosis and cycle-related proteins were detected by Western blot.

### Western Blot

Western blot was done according to our previous study.<sup>17</sup> HCC were treated with CTPG for 24 hours. After washing with ice-cold PBS twice, all adherent and floating cells were collected and lysed in RIPA Lysis Buffer (Beijing ComWin Biotech Co., Ltd) for 20 minutes on ice. After centrifugation at 12000 rpm 4°C for 10 minutes, protein concentration was determined using a Bicinchoninic Acid Assay Kit (Thermo Fisher Scientific, USA) according to the manufacturer's instructions. The same concentration of proteins was separated by 12% SDS-PAGE and transferred to PVDF membranes. After washing with PBST buffer (PBS with 0.05% Tween-20), the membranes were blocked with 5% non-fat milk at 37°C for 1 hour, and then incubated with the primary antibodies (Cell Signaling Technology, MA, USA) at proper dilutions overnight at 4°C. After washing 3 times with PBST, the membrane was incubated with the corresponding HRP-conjugated secondary antibodies (eBioscience) for 2 hours at 37°C. The target proteins were

detected using ECL assay kit (Beyotime). Grayscale scanning data were obtained by Image J.

### Analysis of Mitochondrial Membrane Potential ( $\Delta\psi\text{m}$ )

$\Delta\psi\text{m}$  was determined by membrane-permeable JC-1 dye (Beyotime). Briefly, HepG2 and BEL-7404 cells were treated with different concentrations of CTPG (0, 200, 400, and 600  $\mu\text{g}/\text{mL}$ ) for 24 hours. All cells were collected and washed with JC-1 washing buffer. Cells were stained with the JC-1 fluorescent probe according to manufacturer's instruction for 20 minutes at RT. After washing with PBS twice, all samples were analyzed by flow cytometry (BD FACSCalibur).

### Hoechst 33342 Staining

Hoechst 33342 staining was done according to our previous study.<sup>16</sup> The morphological changes of nuclei were examined using membrane-permeable DNA-binding dye Hoechst 33342 (Beyotime). Briefly, the cells were inoculated in 6-well plate at the concentration of  $1 \times 10^5$  cells/well in 2 mL medium. When reaching 70% to 80% confluence, the cells were treated with 200, 400, and 600  $\mu\text{g}/\text{mL}$  of CTPG or cisplatin for 24 hours. The cells were washed with PBS and fixed with 4% ice-cold paraformaldehyde at 4°C for 10 minutes. After washing with PBS, cells were stained with Hoechst 33342 at 4°C for 10 minutes. Samples were observed by fluorescence inverted microscope (Nikon Eclipse Ti-E, Japan).

### Migration Assay

HCC cell migration was detected through the wound healing assay. In brief, HepG2 cells ( $2 \times 10^4$ /well) were seeded in a 24-well plate. After reaching 80% confluence, the center of each well was scratched once with a 20  $\mu\text{L}$  pipette tip. After washing with PBS, cells were treated with cisplatin (35  $\mu\text{g}/\text{mL}$ ) or different concentrations (0, 200, 400, and 600  $\mu\text{g}/\text{mL}$ ) of CTPG at 37°C. After 24 hours, images of each sample were taken under a microscope (Nikon Eclipse Ti-E). The average distances of cell migration were analyzed by Image J. The percentage of wound healing was calculated by the equation: wound healing (%) =  $(1 - \text{scratch area at indicated time point} / \text{scratch area at 0 hours}) \times 100\%$ . Expression levels of cell migration-related proteins MMP-2 and VEGF were detected by Western blot.

### Proliferation and Apoptosis of Splenocytes

For proliferation analysis, splenocytes were isolated from 3 C57BL/6 mice and stained with CFSE (eBioscience). CFSE labeled cells were inoculated into 24-well



plates at a density of  $2 \times 10^6$  cells in 1 mL medium per well and treated with different concentrations of CTPG (200, 400, and 600  $\mu\text{g}/\text{mL}$ ) or combined with 35  $\mu\text{g}/\text{mL}$  cisplatin for 72 hours. Flow cytometry analysis was performed after staining with CD3-APC and CD19-PE (BD Biosciences). For apoptosis analysis, splenocytes were inoculated into 24-well plates at a density of  $2 \times 10^6$  cells in 1 mL medium per well and treated with different concentrations of CTPG (200, 400, and 600  $\mu\text{g}/\text{mL}$ ) or combined with cisplatin for 24 hours. Flow cytometry analysis were performed after staining with 2.5  $\mu\text{L}$  Annexin V-FITC and 5  $\mu\text{L}$  PI-PE Solution.

### Safety Evaluation and Immunostimulatory Activities of CTPG In Vivo

For evaluating the in vivo immunostimulatory activities of CTPG, 6 to 8 weeks male Kunming mice were randomly divided into 7 groups (5 mice/group). Subcutaneous injection (s.c., 200, 400 mg/kg), intraperitoneal injection (i.p., 200, 400 mg/kg), and intragastric administration (i.g., 200, 400 mg/kg) were applied every 2 days for a total of 7 times, while the control group did not receive any treatment. The mice were weighed every other day and the status of the mice was observed every day. After CTPG treatment, the organs of the mice were separated and weighed. The organ indexes were calculated according to the formula: organ index = organ weight (mg)/body weight (g). The splenocytes were collected, counted and stained with anti-CD3-APC, anti-CD19-PE, anti-CD49b-FITC or anti-CD4-APC, anti-CD44-PE, anti-CD8-FITC (BD Biosciences). Samples were detected by flow cytometry (BD FACSCalibur).

### Antitumor Efficacy of CTPG Combined with Cisplatin in H22 Tumor-Bearing Mice

About 6 to 8 week-old male BALB/c mice were subcutaneously injected with H22 cells ( $1.0 \times 10^6$  per mouse in 100  $\mu\text{L}$  PBS). When the tumor volumes reached approximately 60  $\text{mm}^3$ , tumor-bearing mice were randomly divided into 4 groups (6 mice/group) and treated with cisplatin (4 mg/kg), CTPG (400 mg/kg), cisplatin (4 mg/kg) plus CTPG (400 mg/kg), or without treatment (control group), respectively. Tumor mice were intraperitoneally injected with CTPG on the 5<sup>th</sup>, 7<sup>th</sup>, 9<sup>th</sup>, 11<sup>th</sup>, and 13<sup>th</sup> days, respectively. Cisplatin was intravenously injected on the 7<sup>th</sup> and 11<sup>th</sup> days. The tumor volume and body weight were measured every other day. Tumor volume was calculated as the following: Tumor volume ( $V$ ) =  $a \times b^2/2$ , in which  $a$  and  $b$  represent the longest and shortest diameter of a tumor measured by vernier caliper, respectively. On the 20<sup>th</sup> day, organs and tumors were isolated and weighted. The splenocytes were collected, counted, and

stained with anti-CD3-APC and anti-CD19-PE or anti-CD4-FITC and anti-CD8-APC or anti-CD11b-PE and anti-Gr-1-APC or anti-CD4-FITC, anti-CD25-APC, and anti-Foxp3-PE (BD Biosciences). Subsequently, the frequencies and the numbers of the cells were analyzed by flow cytometry (BD FACSCalibur).

### Statistical Analysis

All data were expressed as mean  $\pm$  standard error of the mean (SEM). Statistical analysis was conducted using one/two-way analysis of variance (ANOVA) using Prism5.0 software.  $P < .05$  was considered statistically significant.

## Results

### CTPG Inhibited the Proliferation of HCC Cells In Vitro

The components of CTPG were qualified and quantified by HPLC using echinacoside and acteoside standards (Supplemental Figure 1A), which were the main components of phenylethanoid glycosides from *Cistanche*.<sup>18</sup> According to the peak retention times and the peak areas, CTPG contained 28% echinacoside and 9.9% acteoside. Besides, the content of polysaccharide in CTPG was 34.8% by phenol-sulfuric acid method.<sup>19</sup> The MTT assay showed that CTPG significantly reduced the viability of BEL-7404 and HepG2 cells in a dose- and time-dependent manner (Figure 1A). Consistently, the proliferation of BEL-7404 cells was significantly inhibited by CTPG treatment, which was analyzed by Ki-67 staining (Figure 1B). The effect of CTPG on the proliferation of splenocytes in vitro was also analyzed by MTT assay. We observed that CTPG enhanced the proliferation of splenocytes in a dose-dependent manner (Figure 1C).

The mitogen-activated protein kinase (MAPK) signaling pathway plays a pivotal role in the survival, differentiation, and drug resistance of human cancer cells.<sup>20</sup> In order to investigate whether the MAPK signaling pathway was involved in the inhibitory effect of CTPG on the proliferation of HCC cells, phosphorylation levels of various proteins from MAPK signal pathway were analyzed in HepG2 cells after treatment with CTPG at different concentrations and different time points. The phosphorylation of JNK (P-JNK) and p38 (P-p38) was dose-dependently enhanced by CTPG treatment. The phosphorylation of ERK (P-ERK) was down-regulated by 200 and 400  $\mu\text{g}/\text{mL}$  CTPG treatment, while P-ERK was up-regulated under 600  $\mu\text{g}/\text{mL}$  CTPG treatment (Figure 1D). Moreover, the levels of P-JNK, P-p38, and P-ERK were up-regulated in a time-dependent way (Figure 1D). These results suggested that CTPG might inhibit the proliferation of HCC cells through the MAPK signaling pathway.

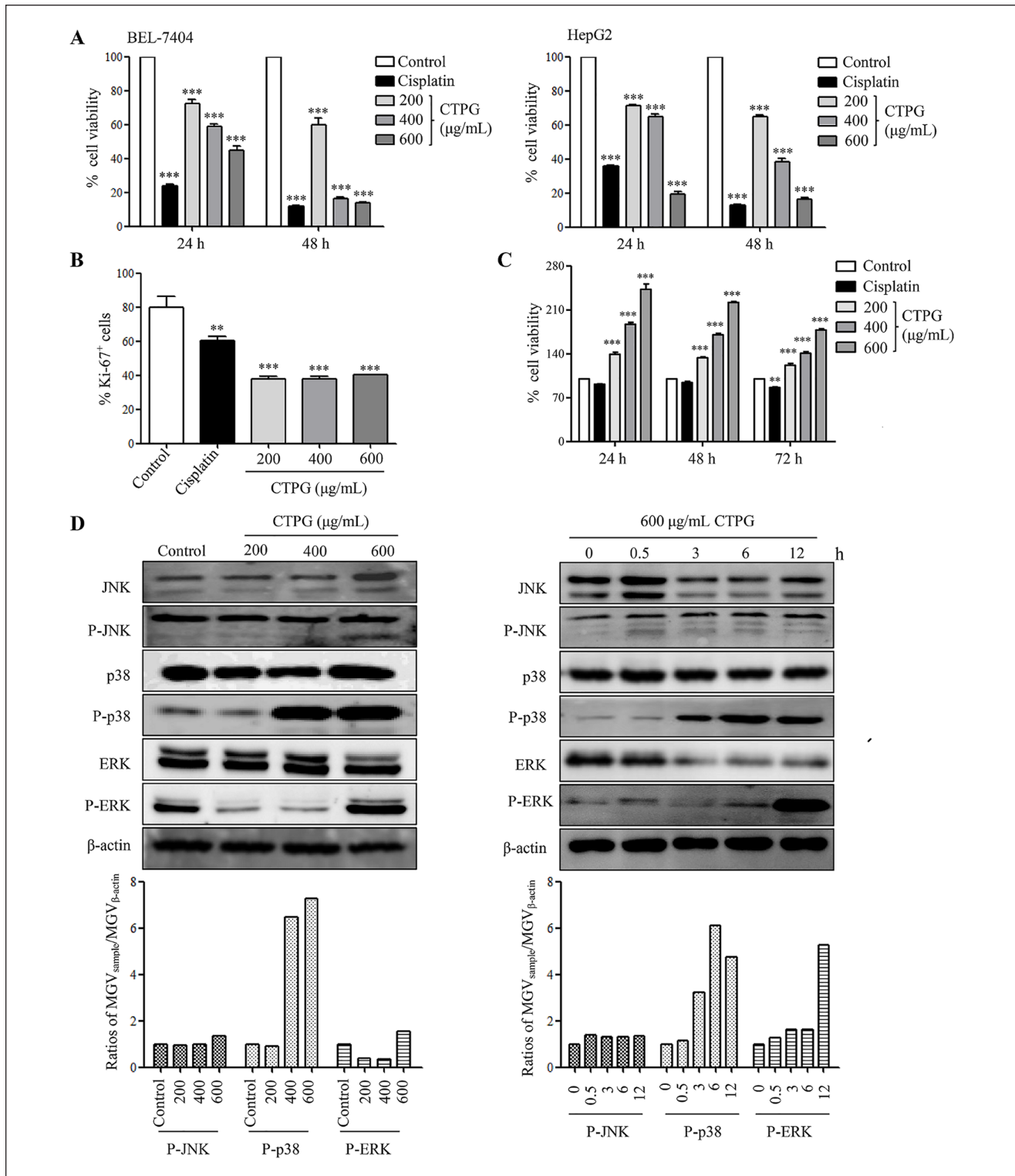


**Figure 1.** The effect of CTPG on the proliferation of HCC cells and splenocytes. (A) BEL-7404 and HepG2 cells were treated by different concentrations (0, 200, 400, 600  $\mu\text{g/mL}$ ) of CTPG for 24 and 48 hours, and then cell viability was detected by MTT assay. (B) BEL-7404 cells were treated with different concentrations of CTPG for 24 hours, and the frequencies of Ki-67<sup>+</sup> cells were detected by flow cytometry. (C) Splenocytes of C57BL/6 mice were treated with different concentrations of CTPG for 24, 48, and 72 hours, and the proliferation was analyzed by MTT assay. Data were analyzed by ANOVA. \*\* $P < .01$ , \*\*\* $P < .001$ , compared with control. (D) HepG2 cells were treated with different concentrations of CTPG for 24 hours or treated with 600  $\mu\text{g/mL}$  CTPG for 0, 0.5, 3, 6, and 12 hours, then proteins were isolated to detect MAPK signaling pathway proteins by Western blot.

### CTPG Induced HCC Cell Cycle Arrest at S Phase

We further analyzed whether CTPG inhibited HCC cell proliferation through induction of cell cycle arrest. After treatment with CTPG, an accumulation of BEL-7404 cells at S-phase was observed in a dose-dependent manner. Similarly, CTPG also induced HepG2 cell cycle arrest at S-phase and the frequencies increased from 40.66% in the control group to 61.90% in the 600  $\mu\text{g}/\text{mL}$  CTPG treated group (Figure 2A). Cyclins and cyclin-dependent kinases (CDKs) play important roles in cell division control and development,<sup>21</sup> which were associated with the G2/M phase.<sup>22</sup> The expression level of Cyclin D1 was dose-dependently decreased by CTPG treatment, but promoted G1 to S phase progression. The expression levels of Cyclin B1, CDK1, and CDK2 were also reduced; these proteins were associated with the G2/M phase (Figure 2B). These results suggested that CTPG suppressed HCC cell proliferation by inducing cell cycle arrest.

### CTPG Activated Mitochondria-Dependent Apoptosis Pathway in HCC Cells

We also detected whether CTPG triggered apoptosis in HCC cells and found that CTPG induced apoptosis in HepG2 and BEL-7404 cells in a dose-dependent manner (Figure 3A). In addition, the expression levels of Bax and Bcl-2 were increased and decreased by CTPG treatment in a dose-dependent manner, respectively (Figure 3B). The apoptosis of HepG2 cells was further determined by Hoechst 33342 staining after treatment with CTPG for 24 hours. The nuclear morphology was observed by inverted fluorescence microscope. As shown in Figure 3C, the control HepG2 cells were homogeneously stained while HepG2 cells treated with CTPG showed chromatin condensation and fragmentation in a dose-dependent manner, which were similar with HepG2 cells treated with cisplatin. These results indicated that CTPG induced apoptosis of HCC cells.

The integrity of the outer mitochondrial membrane is strictly regulated by the Bcl-2 family and the reduction of  $\Delta\psi_m$  promotes the release of cytochrome *c* that activates the caspase cascade to induce apoptosis.<sup>23,24</sup> When  $\Delta\psi_m$  decreases, the JC-1 polymer (red fluorescence) decomposes into monomers (green fluorescence).<sup>25</sup> Therefore, the  $\Delta\psi_m$  of HCC cells was detected by JC-1 staining after CTPG treatment for 24 hours. As shown Figure 4A, the green fluorescence intensity of the FL-1 channel was dose-dependently increased by CTPG treatment while the red fluorescence intensity of the FL-2 channel was dose-dependently decreased in both BEL-7404 and HepG2 cells. Inverted fluorescence microscope observation exhibited a similar result (Figure 4B), indicating that CTPG reduces the  $\Delta\psi_m$  of HCC cells. Subsequently, we observed that levels of

cytochrome *c* were increased in both BEL-7404 and HepG2 cells after CTPG treatment (Figure 4C), which further confirmed the reduction of  $\Delta\psi_m$  in CTPG treated HCC cells.

The release of cytochrome *c* can activate the initiator caspase-9 to induce apoptosis.<sup>26</sup> The results of the Western blot assay suggested that levels of cleaved caspase-3, -7, and -9 were increased while the level of cleaved caspase-8 was not changed (Figure 5). The activated caspase-3 can cleave the DNA repair enzyme of poly (ADP-ribose) polymerase (PARP) to prevent DNA repair and accumulate DNA damage.<sup>27</sup> We also observed up-regulated levels of cleaved PARP. The role of the caspase cascade in HCC cell apoptosis induced by CTPG was further determined by using caspase inhibitor (Z-VAD-FMK) and caspase-3 inhibitor (Ac-DEVD-CHO) respectively. Z-VAD-FMK significantly reversed the apoptosis of BEL-7404 and HepG2 cells induced by CTPG (Supplemental Figure 1B). Similarly, Ac-DEVD-CHO also significantly reversed the apoptosis of HepG2 cells induced by CTPG (Supplemental Figure 1C). The results demonstrated that CTPG induced apoptosis of HCC cells by mitochondria-dependent pathway.

### CTPG Suppressed HCC Cell Migration In Vitro

Cancer cell migration is considered one of the critical processes in tumor metastasis. To determine whether CTPG affects HCC cell migration, HepG2 cell motility was evaluated by the wound-healing assay. As shown in Figure 6A and B, HepG2 cell migration was significantly inhibited by CTPG treatment in a dose-dependent manner. MMP family and VEGF play critical roles in the migration of tumor cells.<sup>28</sup> After CTPG treatment for 24 hours, the levels of MMP-2 and VEGF were significantly decreased (Figure 6C), suggesting that CTPG might suppress the invasion and metastasis of HCC.

### CTPG Enhanced the Immunity of Mice

It has been reported that *Cistanche deserticola* polysaccharides have immunomodulatory functions including promoting lymphocyte proliferation and activating macrophages.<sup>29</sup> T cells and B cells are the main lymphocytes, which mediate cellular and humoral immune responses, respectively. CTPG contained 34.8% polysaccharide content. Therefore, we examined the effects of CTPG on the proliferation of T cells and B cells. As shown in Supplemental Figure 2A, CTPG significantly increased the proliferation of T cells and B cells in a dose-dependent manner, even in the presence of cisplatin. Interestingly, CTPG significantly inhibited the apoptosis of splenocytes induced by cisplatin (Supplemental Figure 2B), indicating that CTPG could ameliorate the side effects of cisplatin on the immune system of mice.

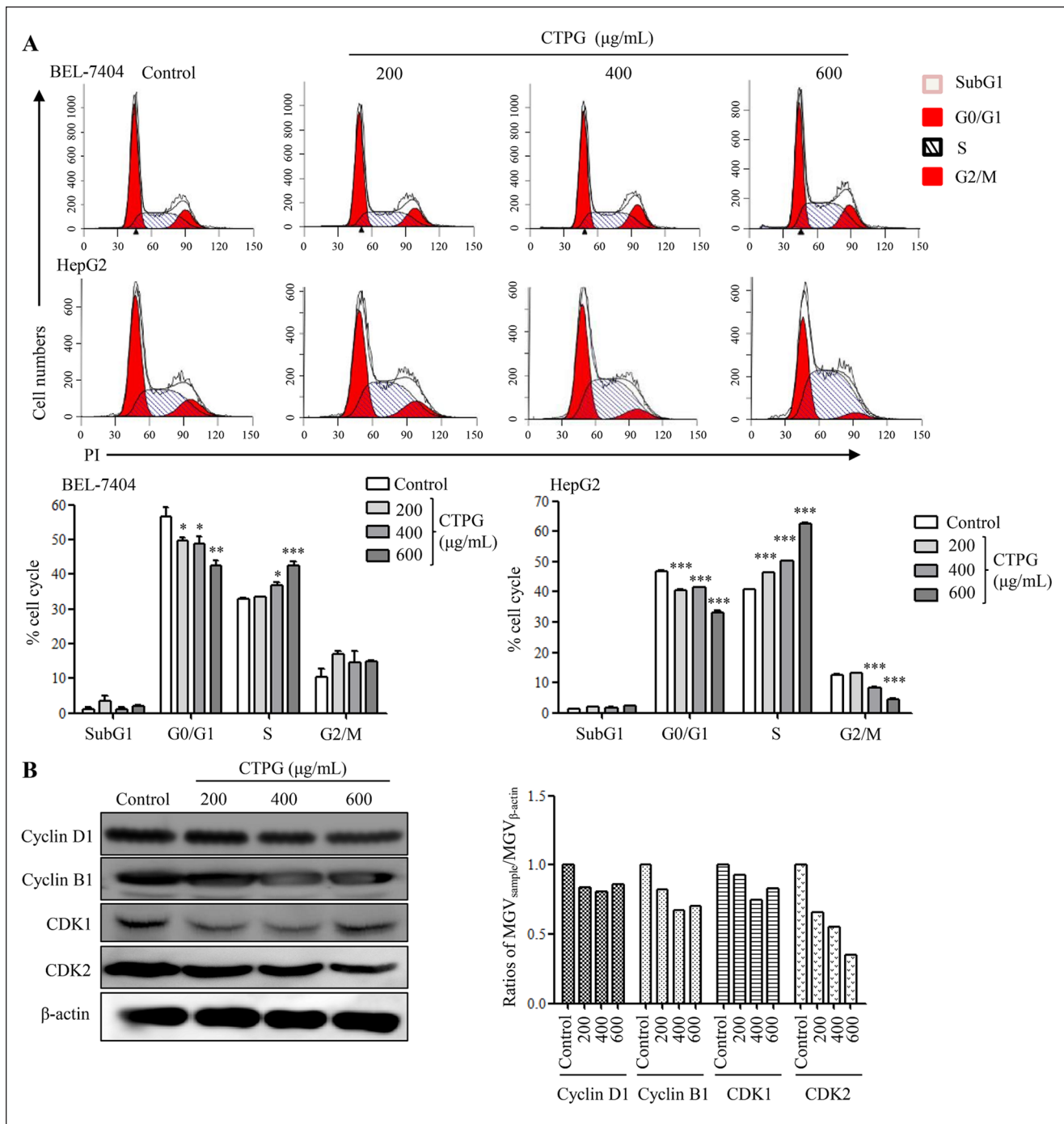


**Figure 2.** The effects of CTPG on cell cycle in HCC cells. (A) BEL-7404 and HepG2 cells were treated with different concentrations (0, 200, 400, 600  $\mu\text{g/mL}$ ) of CTPG for 24 hours. Cell cycle distribution in HCC cells was analyzed by flow cytometry. Data were analyzed by ANOVA. \* $P < .05$ ; \*\* $P < .01$ ; \*\*\* $P < .001$  compared with control. (B) HepG2 cells were treated with different concentration of CTPG for 24 hours, and proteins were isolated to detect the levels of cyclinD1, CDK2, cyclinB1, and CDK1 by Western blot.

We further evaluated the immunostimulatory effect of CTPG on mice. After i.p. injection, s.c. injection and i.g. administration of CTPG (200 and 400 mg/kg), there was no significant change in the state of mice compared with

the untreated group. The body weight of mice also had no significant difference among CTPG-treated groups and untreated group (Figure 7A). The heart, liver, spleen, lung, kidney, and thymus indexes of mice were similar among



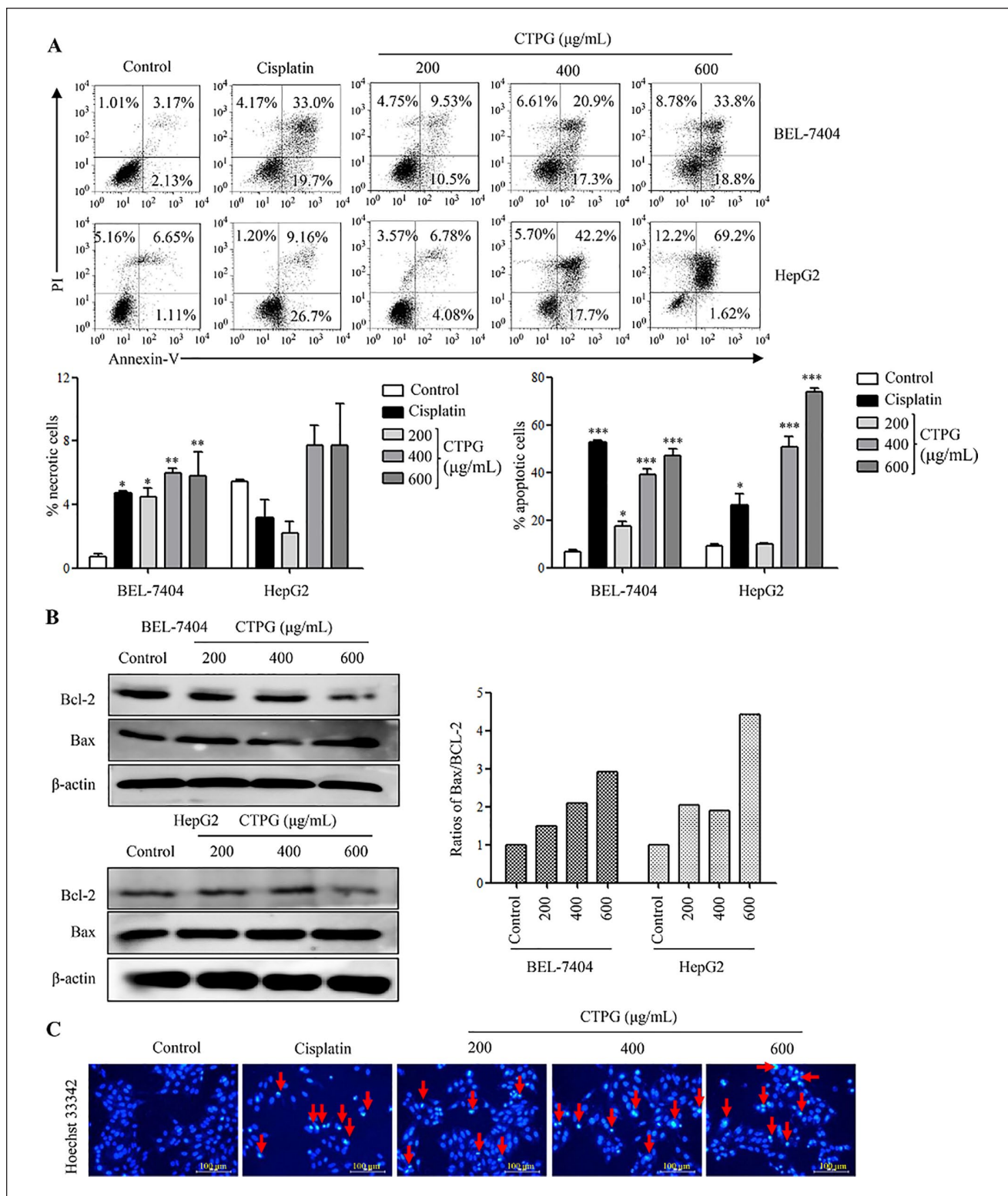


**Figure 3.** The effects of CTPG on apoptosis in HCC cells. Cells were treated with different concentrations (0, 200, 400, 600  $\mu\text{g/mL}$ ) of CTPG for 24 hours. (A) The necrotic and apoptotic BEL-7404 and HepG2 cells were detected by flow cytometry. The upper panel showed the individual dot plots and the lower panel showed the summary data. Data were analyzed by ANOVA. \* $P < .05$ ; \*\* $P < .01$ ; \*\*\* $P < .001$  compared with control. (B) Total protein was isolated to analyze the expressions of Bax and Bcl-2 by Western blot. (C) HepG2 cells were stained with Hoechst 33342 and observed by inverted fluorescence microscopy. The arrows indicated the chromosomal condensation or fragmentation.

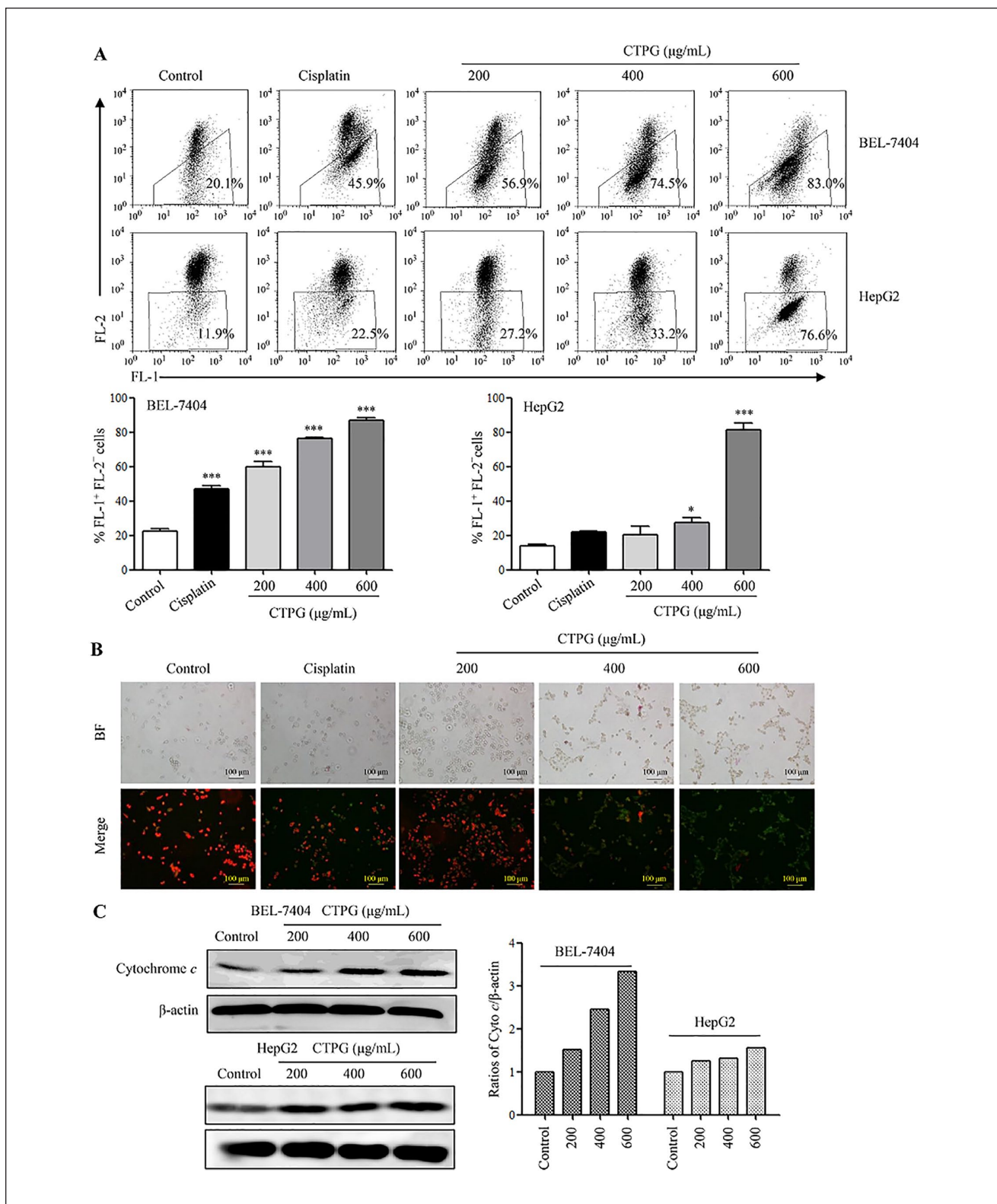


**Figure 4.** The effects of CTPG on  $\Delta\Psi_m$  in HCC cells. BEL-7404 and HepG2 cells were treated with different concentrations (0, 200, 400, 600  $\mu\text{g/mL}$ ) of CTPG. After 24 hours, cells were stained with JC-1 and the fluorescence changes were analyzed by flow cytometry (A) and observed using inverted fluorescence microscopy (B). Data were analyzed by ANOVA. \* $P < .05$ ; \*\*\* $P < .001$  compared with control. (C) After 24 hours, proteins were isolated and the levels of cytochrome c were detected by Western blot.

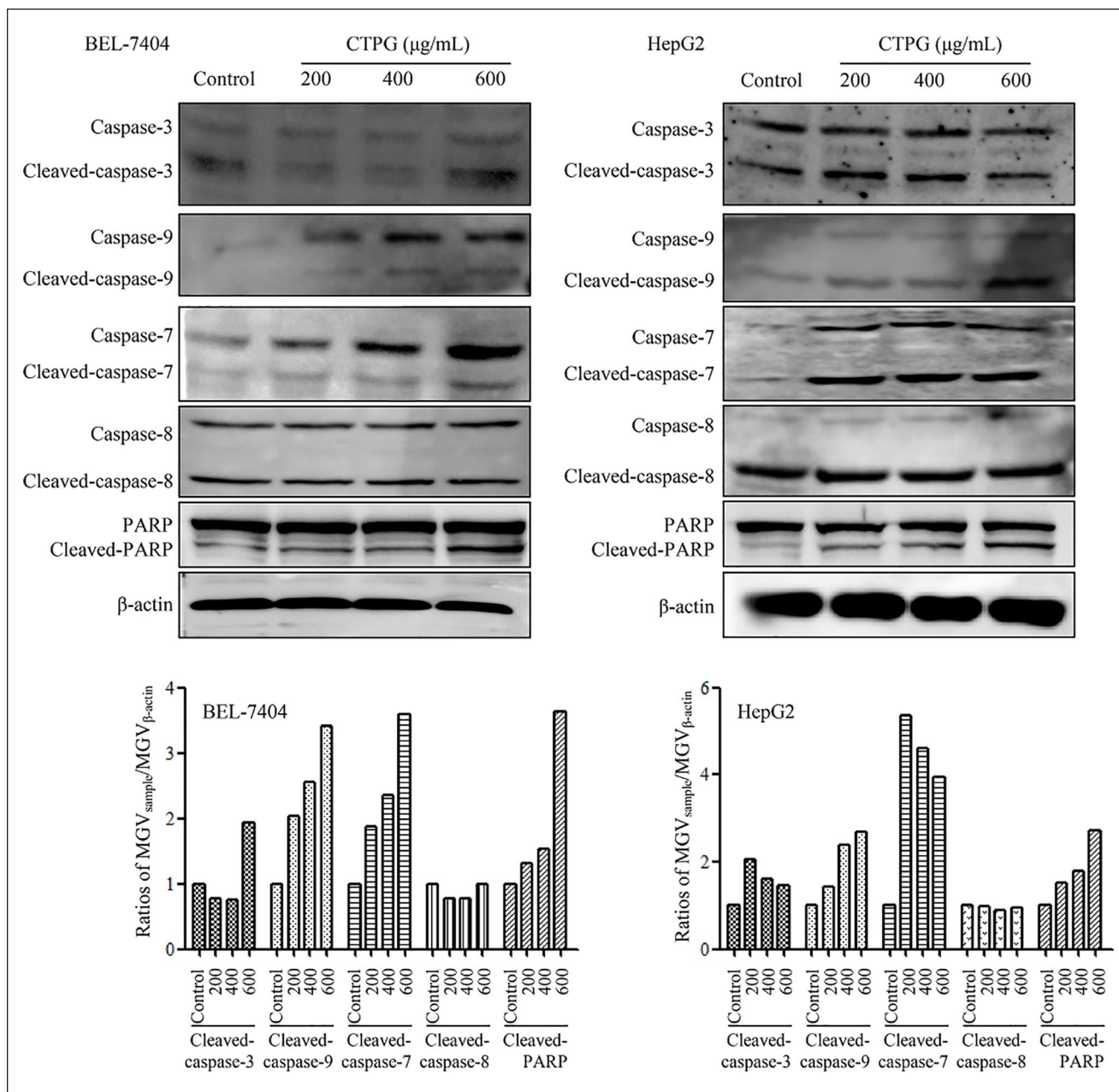


**Figure 5.** CTPG induced apoptosis in HCC cells via caspase pathway. BEL-7404 and HepG2 cells were treated with different concentrations (0, 200, 400, 600 μg/mL) of CTPG. After 24 hours, proteins were isolated and the levels of cleaved caspases and PARP were detected by Western blot.

all groups except the spleen indexes of mice in the 400 mg/kg CTPG i.p. injection group (Table 1). The results suggested that the selected doses of CTPG had no side effect in mice.

The spleen is an important immune defense organ in mammals, and its development directly affects the individual's immune function and the ability to resist diseases. Immune organ index reflects the development and immune function of immune organs. The spleen contains a variety of

immune cells, including T cells, B cells, natural killer cells (NK cells), macrophages, dendritic cells (DCs), and others, which play an important role in the immune system.<sup>30</sup> It had been reported that polysaccharides can increase the number of immune cells to enhance the body's immunity.<sup>31</sup> As i.p. injection of CTPG significantly increased the spleen index (increased 0.55 times), we further analyzed the numbers of various immune cells in spleen. The results showed that i.p. injection of CTPG significantly increased the numbers of T

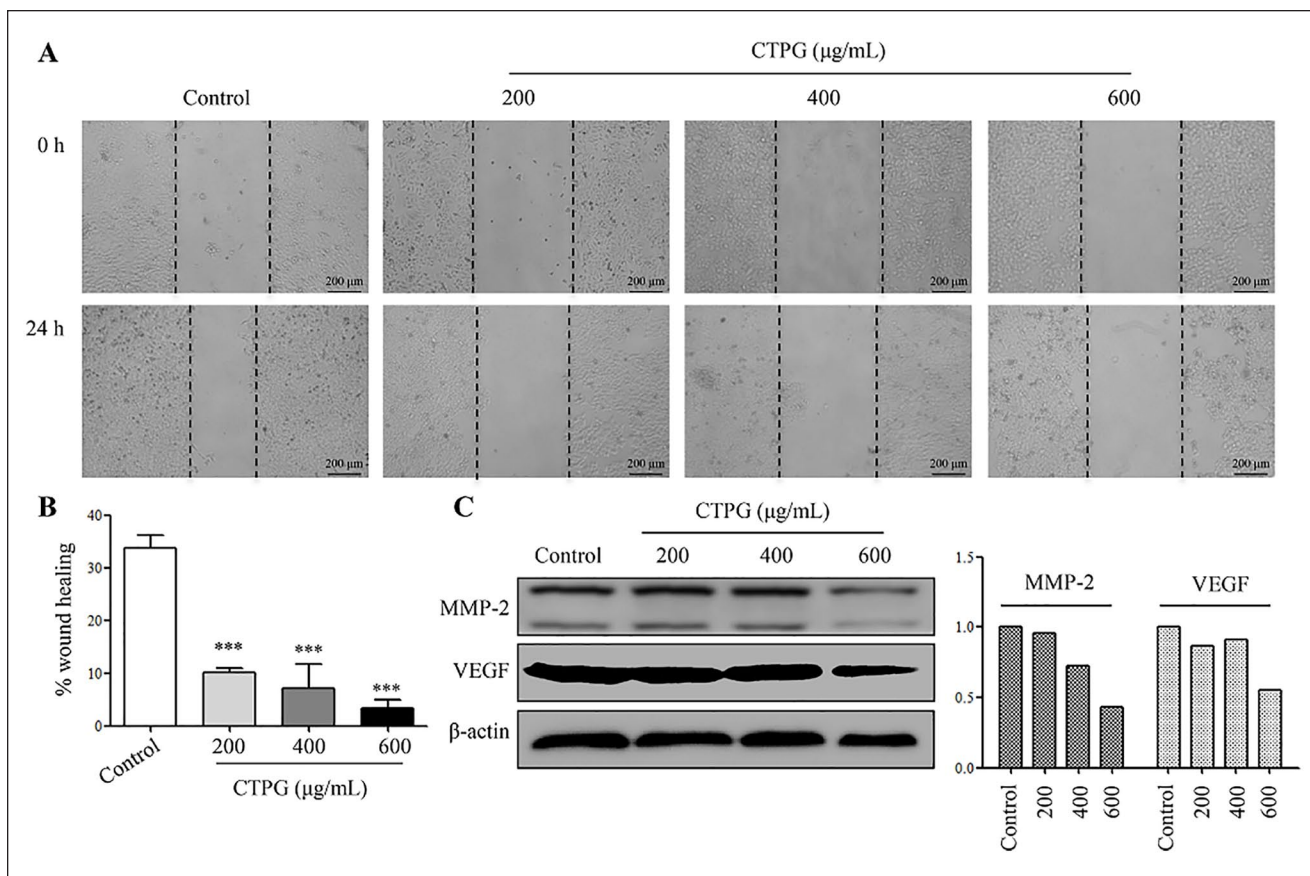


**Figure 6.** CTPG inhibited HCC cell migration in vitro. HepG2 cells were treated with different concentrations (0, 200, 400, 600 µg/mL) of CTPG for 24 hours. HepG2 cell migration was observed by inverted microscope (A) and analyzed by Image J (B). Data were analyzed by ANOVA. \*\*\**P* < .001 compared with control. (C) Proteins were isolated to detect the levels of MMP-2 and VEGF by Western blot.

**Table I.** Organ Indexes of Mice.

Indexes	Untreated	i.p. (mg/kg)		s.c. (mg/kg)		i.g. (mg/kg)	
		200	400	200	400	200	400
Spleen	3.44 ± 0.82	3.98 ± 0.5	5.33 ± 1.18***	3.3 ± 0.4	4.28 ± 0.52	3.45 ± 0.57	3.73 ± 0.32
Heart	5.48 ± 0.61	5.03 ± 0.73	5.42 ± 0.48	5.25 ± 0.75	6.16 ± 0.43	5.16 ± 0.52	4.29 ± 0.35
Liver	77.18 ± 3.81	74.86 ± 5.95	78.94 ± 3.95	70.09 ± 7.99	77.65 ± 4.96	72.69 ± 6.2	72.58 ± 7.37
Lung	9.1 ± 1.85	7.8 ± 0.56	8.77 ± 1.05	9.56 ± 1.1	8.47 ± 1.56	7.47 ± 0.77	8.5 ± 0.51
Kidney	16.06 ± 2.98	13.66 ± 1.05	16.27 ± 1.96	16.42 ± 2.32	16.28 ± 1.25	15.13 ± 1.38	16.83 ± 0.97
Thymus	6.00 ± 0.74	5.65 ± 1.52	5.29 ± 0.6	4.68 ± 1.01	4.5 ± 0.83	5.3 ± 0.86	4.91 ± 0.47

\*\*\**P* < .001 compared with untreated group.

cells (CD3<sup>+</sup>CD19<sup>-</sup> cells) (increased 0.49 times), B cells (CD3<sup>-</sup>CD19<sup>+</sup> cells) (increased 0.49 times) and NK cells (CD3<sup>-</sup>CD19<sup>-</sup>CD49b<sup>+</sup> cells) (increased 1.63 times) compared with the untreated group. CD4<sup>+</sup> and CD8<sup>+</sup> T cells, as the main subtypes of T cells, play an important role in the antigen-specific cellular immune response.<sup>32</sup> Therefore, we further analyzed the number and activation status of CD4<sup>+</sup>

and CD8<sup>+</sup> T cells in the spleen. The results indicated that i.p. injection of CTPG not only significantly increased the numbers of CD4<sup>+</sup> and CD8<sup>+</sup> T cells (increased 0.55 and 0.34 times, respectively) but also enhanced the activation state of CD4<sup>+</sup> T cells (CD4<sup>+</sup>CD44<sup>+</sup> cells) (increased 0.84 times) (Figure 7B), these results suggesting that CTPG had immune enhancement function.



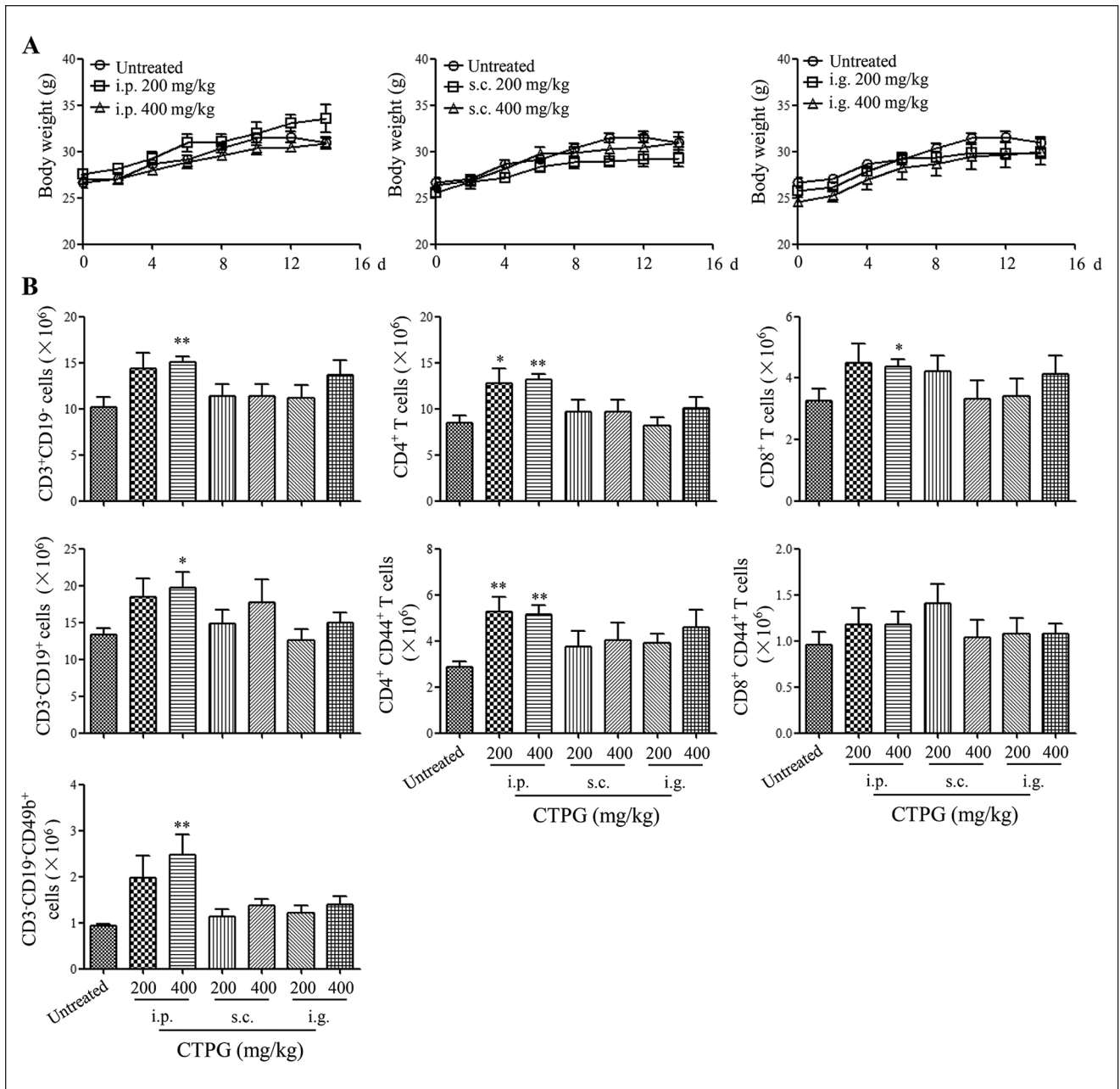


**Figure 7.** The effects of CTPG on immunity of mice. Mice were injected with different concentrations of CTPG through different administration. On day 15, mice were sacrificed to collect spleens. (A) Body weight of mice. (B) The cell numbers in spleens were calculated and the activation of CD4<sup>+</sup> and CD8<sup>+</sup> T cells was detected by flow cytometry. Data were analyzed by ANOVA. \* $P < .05$ ; \*\* $P < .01$  compared with untreated group.

### The Combination of CTPG and Cisplatin Exhibited Potent Antitumor Effect on H22 Tumor Mouse Model

It is generally accepted that chemotherapy or radiotherapy can lead to poor prognosis and induce numerous adverse events, which may be due to the suppression of the immune system and damage to normal tissues and organs.

Polysaccharides from TCM have immune enhancement effects and alleviate the damage of immune organs and immune cells caused by chemotherapy, for example chitosan<sup>33</sup> and *Lycium barbarum* polysaccharides.<sup>34</sup> The above result showed that CTPG could ameliorate the side effects of cisplatin on immune system. Therefore, the antitumor effect of CTPG combined with cisplatin was evaluated in the H22 tumor mouse model. As shown in Figure 8A, CTPG

**Table 2.** Organ Indexes of H22 Tumor-Bearing Mice.

Indexes	Untreated	Cisplatin	CTPG	CTPG + Cisplatin
Spleen	9.99 ± 0.68	7.62 ± 0.68***	11.63 ± 0.80*	8.71 ± 0.90#
Heart	5.67 ± 0.37	6.22 ± 0.59	5.84 ± 0.36	5.32 ± 0.18
Liver	65.38 ± 4.14	72.99 ± 10.37	61.67 ± 1.58	62.29 ± 6.64
Lung	6.39 ± 0.58	7.9 ± 1.10	7.37 ± 1.54	6.07 ± 0.57
Kidney	17.59 ± 0.77	18.62 ± 3.28	17.41 ± 0.84	16.12 ± 1.51
Thymus	1.10 ± 0.09	1.01 ± 0.17	1.14 ± 0.19	0.89 ± 0.11

\* $P < .05$ ; \*\*\* $P < .001$  compared with untreated group; # $P < .05$  compared with cisplatin group.

alone, cisplatin alone and the combination of CTPG and cisplatin (CTPG + cisplatin) significantly suppressed H22 tumor growth compared with the control group. CTPG + cisplatin showed stronger inhibitory effect than that of CTPG and cisplatin alone. On the 20<sup>th</sup> day, the tumor volumes in the control, cisplatin alone, CTPG alone and CTPG + cisplatin groups were about 1707.8, 722.5, 1033.8, and 367.5 mm<sup>3</sup>, respectively. On the same day, the tumors were collected for visual observation (Figure 8B) and weight comparison (Figure 8C). CTPG + cisplatin showed better therapeutic effects on H22 tumor mouse model than CTPG or cisplatin alone. The tumor weight in the CTPG + cisplatin group was lower than that in other groups. These results suggest that the anti-tumor activity of CTPG and cisplatin results in synergistic effects.

The body weights of mice were measured to reflect the health status of mice. The body weight remarkably decreased after cisplatin treatment, suggesting that cisplatin induced severe systemic toxicity.<sup>35</sup> In comparison, CTPG combined with cisplatin significantly ameliorated body weight loss induced by cisplatin, while CTPG alone had no significant effect on mice body weight (Figure 8D). The organs including spleen, heart, liver, lung, kidney, and thymus were also isolated to calculate organ indexes. Compared with the untreated group, spleen indexes were significantly decreased and increased by cisplatin and CTPG, respectively. CTPG + cisplatin recovered spleen indexes compared with cisplatin alone. Other organ indexes showed no significant difference among all groups (Table 2).

### CTPG Combined with Cisplatin Enhanced the Immunity of Tumor Mice

The above results showed that CTPG enhanced the immunity of mice and inhibited the apoptosis of splenocytes induced by cisplatin. We further investigated whether the antitumor effect of CTPG + cisplatin was correlated with enhanced immunity. In the process of tumor occurrence and development, the body's immune system plays an important immune surveillance function, and T cell-mediated cellular immunity plays a key role. CD4<sup>+</sup> T cells have the

function of assisting cellular immunity and humoral immune response, and CD8<sup>+</sup> T cells are the main effector cells of immune response, which can specifically kill target cells and play an important role in tumor immunity and antiviral immunity.<sup>32</sup> The spleens of tumor-bearing mice were collected to detect the numbers of T cells and B cells by flow cytometry. The frequencies and numbers of T cells including CD4<sup>+</sup> and CD8<sup>+</sup> T cells in the CTPG + cisplatin group were significantly higher than those in the control (increased 0.55 and 0.7 times, respectively) and cisplatin groups (increased 0.92 and 1.16 times, respectively) (Figure 9A and B). Compared with the control group, CTPG alone also partly increased the numbers of CD4<sup>+</sup> and CD8<sup>+</sup> T cells although there was no significant difference. The frequencies and numbers of B cells had no significant difference among all groups.

Myeloid-derived suppressor cells (MDSCs) and regulatory T cells (Tregs) expand in tumors and inhibit antitumor immune responses; they suppress the activation and expansion of CD4<sup>+</sup> T cells, the function of effector T cells, the activation and/or proliferation and cytokine formation of CD4<sup>+</sup> and CD8<sup>+</sup> T cells, the B-cell proliferation and immunoglobulin production and class switch, the cytotoxic functions of NK and natural killer T cells (NKT), and the function and maturation of DCs.<sup>36-38</sup> The frequencies and numbers of MDSCs (CD11b<sup>+</sup>Gr-1<sup>+</sup>), macrophages (CD11b<sup>+</sup>Gr-1<sup>-</sup>) and Tregs (natural Tregs: CD4<sup>+</sup>CD25<sup>-</sup>Foxp3<sup>+</sup>; induced Tregs: CD4<sup>+</sup>CD25<sup>+</sup>Foxp3<sup>+</sup>) in the spleens of tumor mice were analyzed by flow cytometry. Compared with the control group, the frequencies and numbers of MDSCs decreased significantly after injection with cisplatin alone (decreased 1.56 times) or in combination with CTPG (decreased 0.62 times). The numbers of CD11b<sup>+</sup>Gr-1<sup>-</sup> macrophages also decreased significantly although there was no significant change in their frequencies (Figure 9C). In addition, CTPG alone and CTPG + cisplatin treatment significantly decreased the frequencies of induced Tregs (decreased 0.33 and 0.37 times, respectively) (Figure 9D). These results suggested that the antitumor effect of CTPG + cisplatin might be correlated with the enhanced immunity characterized by the increased numbers of T cells and the decreased numbers of MDSCs and Tregs.

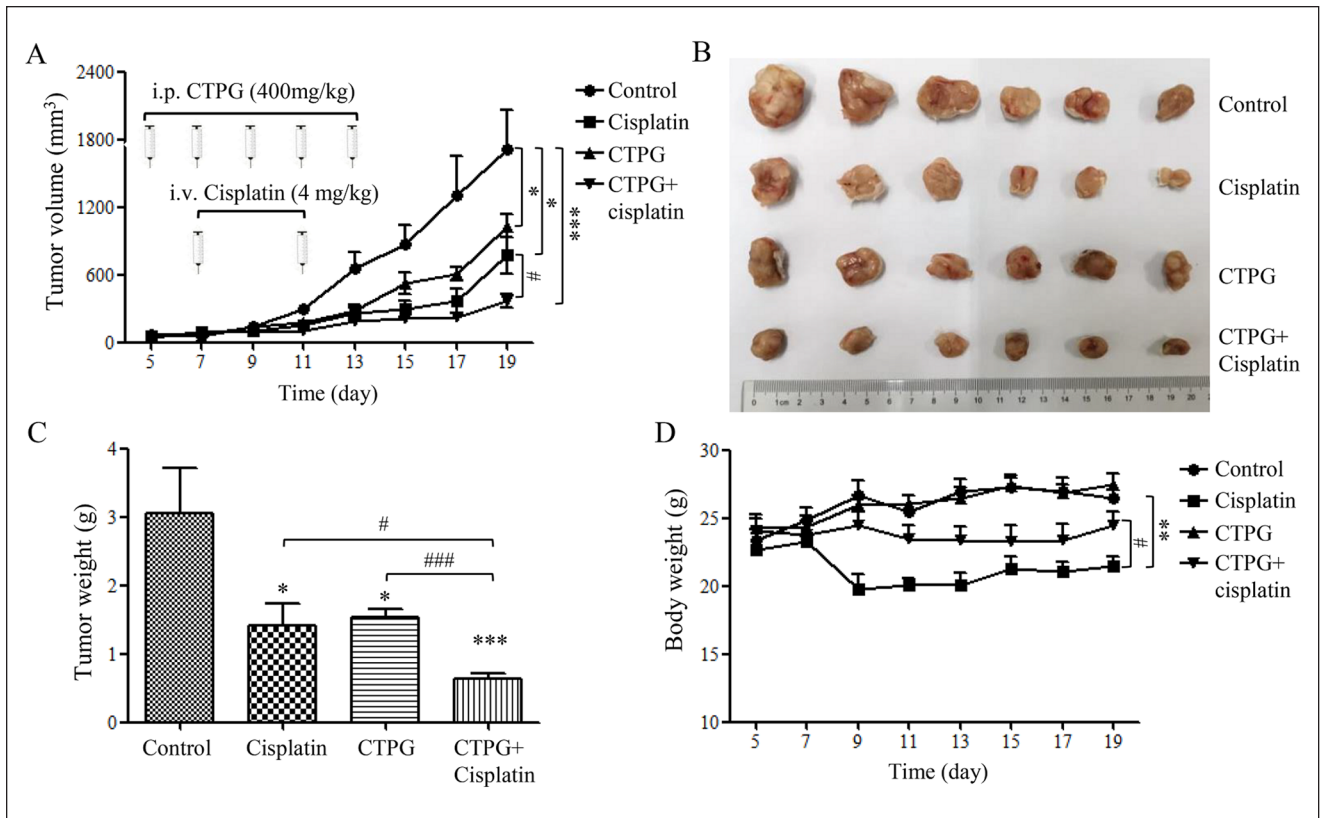


**Figure 8.** Antitumor efficacy of CTPG combined with cisplatin in H22 tumor mouse model. (A) Tumor volumes of mice. The syringe marks represent the day of injection. (B) Photographs of tumors in each group at the end of the experiment. Data were analyzed by two-way ANOVA. (C) Tumor weight of each group at the end of the experiment. (D) Body weight of the mice over the entire experimental period from the day of injection. \* $P < .05$ ; \*\*\* $P < .001$  compared with control group. # $P < .05$ ; ### $P < .001$  compared between experimental groups.

## Discussion

It has been reported that TCM could induce apoptosis of various tumor cells through different pathways, including the extrinsic death receptor, intrinsic mitochondrial and endoplasmic reticulum (ER) stress pathways.<sup>39</sup> Our previous study showed that N-butanol subfraction of *Brassica rapa* L. induced apoptosis of A549 lung adenocarcinoma cells<sup>16</sup> and ethanol extracts of cultivated and wild *Pleurotus ferulae* induced apoptosis of H22 cells via ER stress- and mitochondria-dependent pathway.<sup>17</sup> We also reported that CTPG inhibited the growth of melanoma B16-F10 cells and esophageal carcinoma Eca-109 cells through the induction of apoptosis via a mitochondrial-dependent pathway.<sup>13</sup> Echinacoside is an important compound with many biological activities in PhGs. It had been report that echinacoside exerted its antiproliferative and proapoptotic functions on HepG2 HCC cell line via decreasing TREM2 expression and PI3K/AKT signaling.<sup>40</sup> In the present study, we found that CTPG inhibited the growth of human HCC HepG2 and BEL-7404 cells through activation of the MAPK signaling pathway and induction of apoptosis via

the mitochondria-dependent pathway. Bax and Bcl-2 play a critical role in the mitochondria-dependent apoptosis pathway.<sup>24</sup> Here, we found that CTPG increased the expression of Bax and reduced the expression of Bcl-2 in HepG2 and BEL-7404 cells, which resulted in the reduction of  $\Delta\psi_m$  and the release of cytochrome *c* to activate the caspase cascade. The up-regulated levels of cleaved caspase-9 and cleaved caspase-3 were observed after CTPG treatment, while the levels of cleaved caspase-8 were not changed by CTPG treatment, suggesting that the apoptosis of HepG2 and BEL-7404 cells induced by CTPG was not mediated by the extrinsic signaling pathway. However, our previous study showed that CTPG induced the apoptosis of H22 cells through both intrinsic and extrinsic pathways.<sup>15</sup> These results suggested that CTPG might inhibit the growth of tumor cells through multiple targets and pathways.

TCM has been widely used for treating cancer through multiple signal pathways with or without minor side effects.<sup>41</sup> The MAPK signaling pathway is closely related to the occurrence, invasion and metastasis of tumor cells, which mainly involves p38 pathway, JNK/SAPK pathway

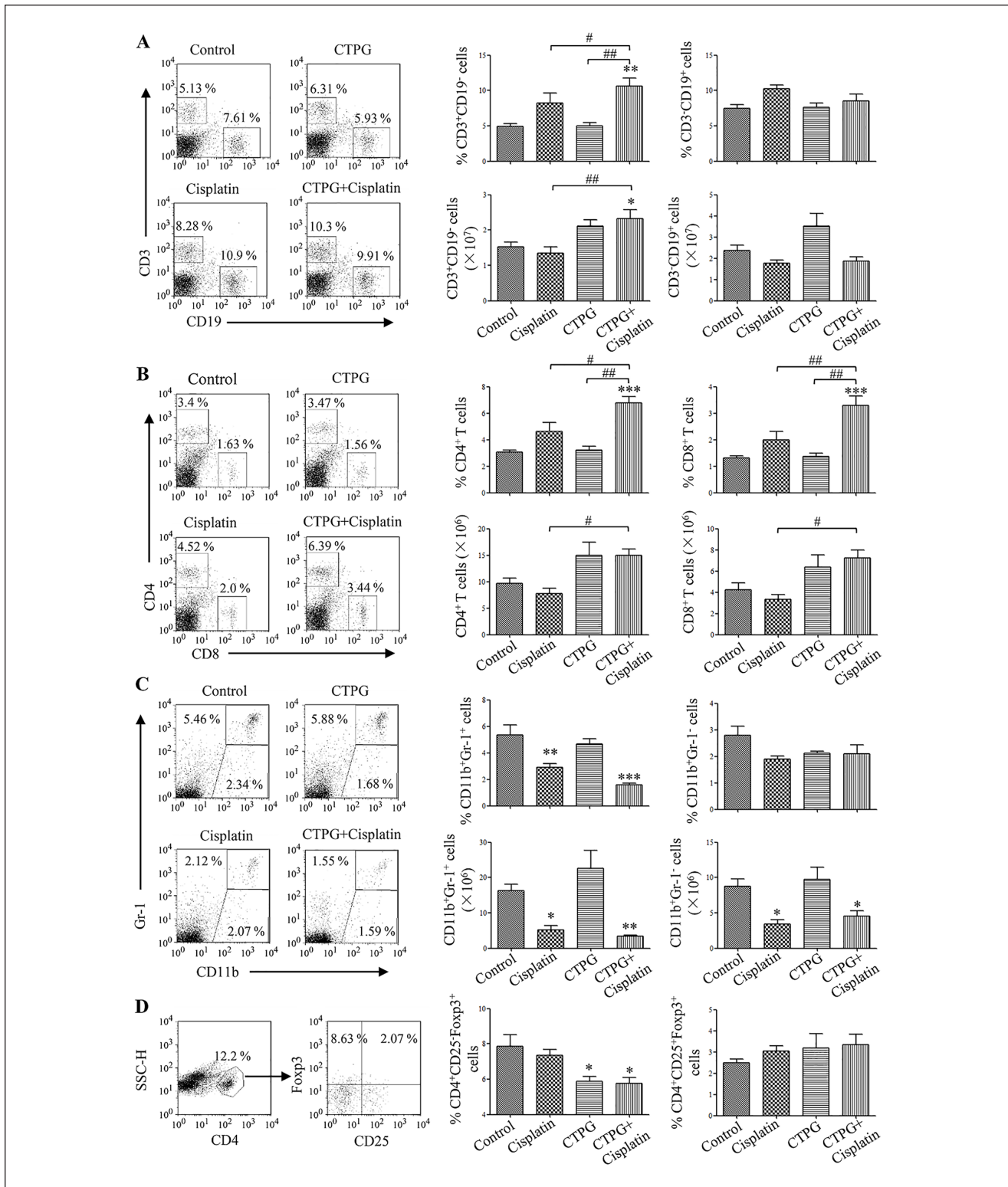


**Figure 9.** The effects of combined therapy on immunity of tumor-bearing mice. Spleens of tumor mice were isolated to detect the frequencies and numbers of immune cells at the end of experiment. (A) The frequencies and numbers of T and B cells. (B) The frequencies and numbers of CD4<sup>+</sup> and CD8<sup>+</sup> T cells. (C) The frequencies and numbers of MDSCs (CD11b<sup>+</sup>Gr-1<sup>+</sup>) and macrophages (CD11b<sup>+</sup>Gr-1<sup>-</sup>). (D) The frequencies of Tregs. Data were analyzed by two-way ANOVA. \* $P < .05$ ; \*\* $P < .01$ ; \*\*\* $P < .001$  compared with control group. # $P < .05$ ; ## $P < .01$  compared between experimental groups.



and ERK1/2 pathway.<sup>20</sup> The activation of p38 and JNK can induce apoptosis but the activation of ERK1/2 can be anti-apoptotic or pro-apoptotic depending on the cell properties.<sup>42</sup> It has been reported that CHM induced the apoptosis of tumor cells by activating the p38, JNK, or ERK MAPK pathways.<sup>43,44</sup> We found that CTPG up-regulated the phosphorylated levels of p38, JNK, and ERK, suggesting that the MAPK signaling pathway might be involved in the apoptosis of HCC cells induced by CTPG.

Chemotherapy and radiotherapy can cause various adverse events including the suppression of the immune system. In order to improve the clinical efficacy of chemotherapy, natural polysaccharides have been approved to be used as adjuvants for cancer treatment. It has been reported that the combination of lentinan and the chemotherapeutic agent tegafur improved the clinical efficacy of patients with esophageal carcinoma through enhancing the patient's immune function.<sup>45</sup> In our previous studies, the in vivo inhibitory effect of CTPG on tumor growth is related to not only its direct antitumor effect but also its immune enhancement function.<sup>13,15</sup> The immune enhancement function of CTPG might be correlated with its polysaccharide content. Here, the in vivo antitumor effect of CTPG + cisplatin was investigated. In the H22 tumor mouse model, CTPG + cisplatin not only showed the best antitumor effect but also reduced the side effects of cisplatin. CTPG + cisplatin enhanced the immunity of tumor-bearing mice through increasing the numbers of CD4<sup>+</sup> and CD8<sup>+</sup> T cells and decreasing the numbers of MDSCs and Tregs, which participated in the tumor-induced inhibitory microenvironment, promoted tumor growth, and inhibited immune response.<sup>46</sup> The increased numbers of T cells might be corrected with their proliferation promoted by CTPG and their decreased apoptosis protected by CTPG. However, the mechanisms of CTPG to reduce the numbers of MDSCs and Tregs need further investigation.

In conclusion, CTPG induced apoptosis in HCC cells through both the mitochondria-dependent and MAPK signaling pathways in vitro and inhibited the growth of HCC through direct antitumor effects and indirect immune enhancement in combination with cisplatin. CTPG might serve as a potential candidate for the treatment of HCC.

### Author Contributions

P.Y., C.F., Y.Y., A.A., F.Z., and X.W. performed experiments. W.W., J.L., and Y.L. analyzed data and prepared figures. L.X. and J.L. designed the experiments and wrote the manuscript. All authors reviewed the manuscript.

### Declaration of Conflicting Interests

The author(s) declared no potential conflicts of interest with respect to the research, authorship, and/or publication of this article.

### Funding

The author(s) disclosed receipt of the following financial support for the research, authorship, and/or publication of this article: This work was supported by the National Natural Science Foundation of China (U1803381 to Jinyao Li and 31860258 to Lijie Xia), and the Doctoral Start-up Foundation of Xinjiang University (BS180222).

### Ethics Approval and Consent to Participate

The experimental protocol was approved by the Committee on the Ethics of Animal Experiments of Xinjiang Key Laboratory of Biological Resources and Genetic Engineering (BRGE-AE001).

### ORCID iD

Lijie Xia  <https://orcid.org/0000-0002-0411-246X>

### Supplemental Material

Supplemental material for this article is available online.

### References

1. Bray F, Ferlay J, Soerjomataram I, Siegel RL, Torre LA, Jemal A. Global cancer statistics 2018: GLOBOCAN estimates of incidence and mortality worldwide for 36 cancers in 185 countries. *CA Cancer J Clin.* 2018;68:394-424.
2. Chen W, Zheng R, Baade PD, et al. Cancer statistics in China, 2015. *CA Cancer J Clin.* 2016;66:115-132.
3. Forner A, Reig ME, de Lope CR, Bruix J. Current strategy for staging and treatment: the BCLC update and future prospects. *Semin Liver Dis.* 2010;30:61-74.
4. European Association For The Study Of The Liver; European Organisation For Research And Treatment Of Cancer. EASL-EORTC clinical practice guidelines: management of hepatocellular carcinoma. *J Hepatol.* 2012;56:908-943.
5. Omata M, Lesmana LA, Tateishi R, et al. Asian Pacific Association for the Study of the Liver consensus recommendations on hepatocellular carcinoma. *Hepatol Int.* 2010;4:439-474.
6. Zhu YJ, Zheng B, Wang HY, Chen L. New knowledge of the mechanisms of sorafenib resistance in liver cancer. *Acta Pharmacol Sin.* 2017;38:614-622.
7. Yang Z, Liao X, Lu Y, et al. Add-on therapy with traditional Chinese medicine improves outcomes and reduces adverse events in hepatocellular carcinoma: a meta-analysis of randomized controlled trials. *Evid Based Complement Alternat Med.* 2017;2017:3428253.
8. Shi Z, Song T, Wan Y, et al. A systematic review and meta-analysis of traditional insect Chinese medicines combined chemotherapy for non-surgical hepatocellular carcinoma therapy. *Sci Rep.* 2017;7:4355.
9. Wu CR, Lin HC, Su MH. Reversal by aqueous extracts of *Cistanche tubulosa* from behavioral deficits in Alzheimer's disease-like rat model: relevance for amyloid deposition and central neurotransmitter function. *BMC Complement Altern Med.* 2014;14:202.
10. Nan ZD, Zeng KW, Shi SP, Zhao MB, Jiang Y, Tu PF. Phenylethanoid glycosides with anti-inflammatory activities

- from the stems of *Cistanche deserticola* cultured in Tarim desert. *Fitoterapia*. 2013;89:167-174.
11. Jiang Y, Tu PF. Analysis of chemical constituents in *Cistanche* species. *J Chromatogr A*. 2009;1216:1970-1979.
  12. Morikawa T, Pan Y, Ninomiya K, et al. Acylated phenylethanoid oligoglycosides with hepatoprotective activity from the desert plant *Cistanche tubulosa*. *Bioorg Med Chem*. 2010;18:1882-1890.
  13. Li J, Li J, Aipire A, et al. Phenylethanoid glycosides from *Cistanche tubulosa* inhibits the growth of B16-F10 cells both in vitro and in vivo by induction of apoptosis via mitochondria-dependent pathway. *J Cancer*. 2016;7:1877-1887.
  14. Fu C, Li J, Aipire A, et al. *Cistanche tubulosa* phenylethanoid glycosides induce apoptosis in Eca-109 cells via the mitochondria-dependent pathway. *Oncol Lett*. 2019;17:303-313.
  15. Yuan P, Li J, Aipire A, et al. *Cistanche tubulosa* phenylethanoid glycosides induce apoptosis in H22 hepatocellular carcinoma cells through both extrinsic and intrinsic signaling pathways. *BMC Complement Altern Med*. 2018;18:275.
  16. Aipire A, Chen Q, Cai S, et al. N-butanol subfraction of *Brassica Rapa L.* promotes reactive oxygen species production and induces apoptosis of A549 lung adenocarcinoma cells via mitochondria-dependent pathway. *Molecules*. 2018;23:1687.
  17. Yang Y, Yuan P, Wei X, et al. Cultivated and wild *Pleurotus ferulae* ethanol extracts inhibit hepatocellular carcinoma cell growth via inducing endoplasmic reticulum stress- and mitochondria-dependent apoptosis. *Sci Rep*. 2018;8:13984.
  18. Jiang Y, Li SP, Wang YT, Chen XJ, Tu PF. Differentiation of *Herba Cistanches* by fingerprint with high-performance liquid chromatography-diode array detection-mass spectrometry. *J Chromatogr A*. 2009;1216:2156-2162.
  19. Masuko T, Minami A, Iwasaki N, Majima T, Nishimura S, Lee YC. Carbohydrate analysis by a phenol-sulfuric acid method in microplate format. *Anal Biochem*. 2005;339:69-72.
  20. De Luca A, Maiello MR, D'Alessio A, Pergameno M, Normanno N. The RAS/RAF/MEK/ERK and the PI3K/AKT signalling pathways: role in cancer pathogenesis and implications for therapeutic approaches. *Expert Opin Ther Targets*. 2012;16:S17-S27.
  21. Lee Y, Lahens NF, Zhang S, Bedont J, Field JM, Sehgal A. G1/S cell cycle regulators mediate effects of circadian dysregulation on tumor growth and provide targets for timed anti-cancer treatment. *PLoS Biol*. 2019;17:e3000228.
  22. Gao SY, Li J, Qu XY, Zhu N, Ji YB. Downregulation of Cdk1 and cyclinB1 expression contributes to oridonin-induced cell cycle arrest at G2/M phase and growth inhibition in SGC-7901 gastric cancer cells. *Asian Pac J Cancer Prev*. 2014;15:6437-6441.
  23. Zamzami N, Marchetti P, Castedo M, et al. Reduction in mitochondrial potential constitutes an early irreversible step of programmed lymphocyte death in vivo. *J Exp Med*. 1995;181:1661-1672.
  24. Martinou JC, Youle RJ. Mitochondria in apoptosis: Bcl-2 family members and mitochondrial dynamics. *Dev Cell*. 2011;21:92-101.
  25. Chong ZZ, Lin SH, Li F, Maiese K. The Sirtuin Inhibitor Nicotinamide Enhances Neuronal Cell Survival During Acute Anoxic Injury Through AKT, BAD, PARP, and Mitochondrial Associated "Anti-Apoptotic" Pathways. *Curr Neurovasc Res*. 2005;2:271-285.
  26. Lee YJ, Lee C. Porcine deltacoronavirus induces caspase-dependent apoptosis through activation of the cytochrome c-mediated intrinsic mitochondrial pathway. *Virus Res*. 2018;253:112-123.
  27. Rancourt A, Satoh MS. Delocalization of nucleolar poly(ADP-ribose) polymerase-1 to the nucleoplasm and its novel link to cellular sensitivity to DNA damage. *DNA Repair (Amst)*. 2009;8:286-297.
  28. Liu QH, Wang Y, Yong HM, et al. XRCC1 serves as a potential prognostic indicator for clear cell renal cell carcinoma and inhibits its invasion and metastasis through suppressing MMP-2 and MMP-9. *Oncotarget*. 2017;8:109382-109392.
  29. Dong Q, Yao J, Fang JN, Ding K. Structural characterization and immunological activity of two cold-water extractable polysaccharides from *Cistanche deserticola* Y. C. Ma. *Carbohydr Res*. 2007;342:1343-1349.
  30. Smith KG, Hunt JL. On the use of spleen mass as a measure of avian immune system strength. *Oecologia*. 2004;138:28-31.
  31. Kikete S, Luo L, Jia B, Wang L, Ondieki G, Bian Y. Plant-derived polysaccharides activate dendritic cell-based anti-cancer immunity. *Cytotechnology*. 2018;70:1097-1110.
  32. Miyara M, Sakaguchi S. Natural regulatory T cells: mechanisms of suppression. *Trends Mol Med*. 2007;13:108-116.
  33. Zhai X, Yang X, Zou P, et al. Protective Effect of chitosan oligosaccharides against cyclophosphamide-induced immunosuppression and irradiation injury in mice. *J Food Sci*. 2018;83:535-542.
  34. Yang DM, Zhang JQ, Fei YF. *Lycium barbarum* polysaccharide attenuates chemotherapy-induced ovarian injury by reducing oxidative stress. *J Obstet Gynaecol Res*. 2017;43:1621-1628.
  35. Zhu J, Xu J, Jiang LL, et al. Improved antitumor activity of cisplatin combined with *Ganoderma lucidum* polysaccharides in U14 cervical carcinoma-bearing mice. *Kaohsiung J Med Sci*. 2019;35:222-229.
  36. Gabrilovich DI, Nagaraj S. Myeloid-derived suppressor cells as regulators of the immune system. *Nat Rev Immunol*. 2009;9:162-174.
  37. Kryczek I, Liu R, Wang G, et al. FOXP3 defines regulatory T cells in human tumor and autoimmune disease. *Cancer Res*. 2009;69:3995-4000.
  38. Nagaraj S, Gupta K, Pisarev V, et al. Altered recognition of antigen is a mechanism of CD8<sup>+</sup> T cell tolerance in cancer. *Nat Med*. 2007;13:828-835.
  39. Peng KZ, Ke Y, Zhao Q, et al. OP16, a novel ent-kaurene diterpenoid, potentiates the antitumor effect of rapamycin by inhibiting rapamycin-induced feedback activation of Akt signaling in esophageal squamous cell carcinoma. *Biochem Pharmacol*. 2017;140:16-27.
  40. Ye Y, Song Y, Zhuang J, Wang G, Ni J, Xia W. Anticancer effects of echinacoside in hepatocellular carcinoma mouse model and HepG2 cells. *J Cell Physiol*. 2019;234:1880-1888.
  41. Yan Z, Lai Z, Lin J. Anticancer properties of traditional Chinese medicine. *Comb Chem High Throughput Screen*. 2017;20:423-429.

42. Yang Y, Zhu X, Chen Y, Wang X, Chen R. p38 and JNK MAPK, but not ERK1/2 MAPK, play important role in colchicine-induced cortical neurons apoptosis. *Eur J Pharmacol.* 2007;576:26-33.
43. Chou SM, Lai WJ, Hong T, et al. Involvement of p38 MAPK in the anticancer activity of cultivated cordyceps militaris. *Am J Chin Med.* 2015;43:1043-1057.
44. Wong DJ, Robert L, Atefi MS, et al. Erratum to: antitumor activity of the ERK inhibitor SCH722984 against BRAF mutant, NRAS mutant and wild-type melanoma. *Mol Cancer.* 2015;14:128.
45. Wang JL, Bi Z, Zou JW, Gu XM. Combination therapy with lentinan improves outcomes in patients with esophageal carcinoma. *Mol Med Rep.* 2012;5:745-748.
46. Kobayashi A, Weinberg V, Darragh T, Smith-McCune K. Evolving immunosuppressive microenvironment during human cervical carcinogenesis. *Mucosal Immunol.* 2008;1: 412-420.